Konya Mühendislik Bilimleri Dergisi, c. 13, s. 1, 180-203, 2025
Konya Journal of Engineering Sciences, v. 13, n. 1, 180-203, 2025
ISSN: 2667-8055 (Electronic)
DOI: 10.36306/konjes.1569087

OPTIMIZATION OF SHEAR AND PEEL STRESSES IN DOUBLE-L-BRACKET JOINTS USING RESPONSE SURFACE METHODOLOGY

*** Bertan BEYLERGİL**

Alanya Alaaddin Keykubat University, Engineering Faculty, Mechanical Engineering Department, Alanya, TÜRKİYE
bertan.beylergil@alanya.edu.tr

Highlights

- Optimized shear and peel stresses in double-L-bracket joints using RSM.
- Key factors: joint height, arm lengths, adhesive thickness, shear, and peel forces.
- Reduced L2 and increased Tg minimized both shear and peel stresses effectively.
- Box-Behnken Design generated predictive models with high accuracy (99.8% variance).
- Findings offer design insights for stronger adhesive joints.

***Corresponding Author:** Bertan BEYLERGİL, bertan.beylergil@alanya.edu.tr

Konya Mühendislik Bilimleri Dergisi, c. 13, s. 1, 180-203, 2025
Konya Journal of Engineering Sciences, v. 13, n. 1, 180-203, 2025
ISSN: 2667-8055 (Electronic)
DOI: 10.36306/konjes.1569087

OPTIMIZATION OF SHEAR AND PEEL STRESSES IN DOUBLE-L-BRACKET JOINTS USING RESPONSE SURFACE METHODOLOGY

*** Bertan BEYLERGİL**

Alanya Alaaddin Keykubat University, Engineering Faculty, Mechanical Engineering Department, Alanya, TÜRKİYE
bertan.beylergil@alanya.edu.tr

(Received: 17.10.2024; Accepted in Revised Form: 07.02.2025)

ABSTRACT: This study aims to optimize the design parameters of a double-L-bracket joint using an analytical approach combined with Response Surface Methodology (RSM). The focus is on minimizing the joint's shear and peel stresses, which are critical for adhesive joint integrity. A Bigwood & Crocombe analytical model was employed to simulate the stress distributions in the joint under various geometrical configurations and loading conditions. Six factors, including joint height (H), vertical arm length (L1), horizontal arm length (L2), adhesive thickness (Tg), shear force (Fx), and peel force (Fz), were analyzed. A Box-Behnken Design (BBD) was used to generate 54 configurations, and the resulting stress responses were modeled through quadratic regression models. The analysis reveals that horizontal arm length (L2), adhesive thickness (Tg), and applied forces (Fx and Fz) significantly influence the stress levels in the joint. The optimization results indicate that reducing L2 and increasing Tg can effectively minimize both shear and peel stresses. The optimized configuration achieves a peel stress of 1.450 MPa and a shear stress of 2.120 MPa, both of which align closely with analytical predictions. The close agreement between RSM-based predictions and analytical calculations validates the robustness of the model. This optimization provides valuable insights for improving the structural performance of adhesive joints in practical applications.

Keywords: *Response Surface Methodology (RSM), Box-Behnken Design (BBD), Adhesive Joint Optimization, Double-L-Bracket Joint*

1. INTRODUCTION

The adhesive bonding technique, a cornerstone of modern engineering, presents enormous advantages in such ways that it can join dissimilar materials, distribute loads in a more uniform manner than that of mechanical fasteners, reducing stress concentration. However, complexity, especially its inherent susceptibility to peel and shear stresses, demands great understanding and optimization of the joints to ensure structural integrity and longevity. With the demands on lightweight and high-performance structures in aerospace, automotive, and civil engineering applications, there is an increasing need for optimization of adhesive bonding [1-3].

In the process of optimizing and evaluating adhesive bonding, statistical methodologies have proved to be very important tools for engineers to investigate complex design spaces while highlighting the most feasible bonding configuration. While these methods improve mechanical performance in adhesive joints, they also have a tendency to give highly reduced material consumption and manufacturing costs, hence being greatly advantageous in both academic research and industrial applications. These approaches permit the determination of the bonding conditions which minimize the risk of failure, by systematically exploring a number of design factors such as adhesive thickness and overlap length, including material properties.

***Corresponding Author:** Bertan BEYLERGİL, bertan.beylergil@alanya.edu.tr

For example, da Silva et al. [4] took a statistical approach by using the Taguchi method to investigate adhesive type and thickness on lap shear strength in single-lap joints. The authors could quantify the relative importance of these variables by testing three adhesives with distinct levels of ductility and three different bondline thicknesses: 0.2 mm, 0.5 mm, and 1 mm. The ANOVA test showed adhesive thickness and toughness to be the most influencing factors on joint strength, with adhesive thickness having a slightly higher effect. The statistical approach yielded a predictive model for lap shear strength based on the properties of adhesives. In a similar vein, Kim et al. [5] coupled the mixed-mode continuum damage model with the Taguchi method and Response Surface Methodology (RSM) to investigate the failure characteristics of functionally graded adhesive bonded joints. Their analysis identified the adhesive shear strength as the most influential factor on failure load, and RSM was used in developing a predictive model that determines the optimal parameters to enhance joint load-bearing capacity.

In another research, Vieira et al. [6] employed the Taguchi method for optimizing tensile performance in adhesively bonded rod-tube joints. The study investigated geometric factors such as overlap length, tube thickness, rod diameter, and adhesive fillet angle, and also investigated adhesive type. ANOVA described overlap length and adhesive type as the most important variables affecting performance. The Taguchi method reduced the number of experiments, and this research is far more effective in analyzing each factor's effect on joint strength, arriving at an optimum design for structural applications. Similarly, Mandolfino et al. [7] applied RSM combined with a Face-centered Central Composite Design to investigate the optimization of adhesive bonding in pulsed laser-treated CFRP composites. The statistical methodology pursued the best parameters for laser treatment concerning power, pitch, and lateral overlap affecting the TSS of adhesive joints. Using ANOVA, the significance of each factor and their interactions was tested, after which statistical models useful in the prediction of joint performance against parameter combinations that have not been previously tested were developed, hence optimizing the process at reduced energy consumption.

The effect that adhesive thickness has on the mechanical performance and reliability of structural adhesive joints was studied by Arenas et al. [8] using statistical techniques based on the Weibull distribution. The tensile shear strength they analyzed with respect to different thicknesses of adhesives indicated that thinner adhesives, in general, may develop a higher strength due to fewer defects. In another study, Wang and Zeng [9] utilized RSM with the Box-Behnken design in the optimization of particle-reinforced adhesive joints. ANOVA was done to check parameters like the size of the particles, thickness of the adhesive layer, and mass fraction in respect of failure load and energy absorption. The results indicated that the particle size had the most significant impact on failure loading, while mass fraction represented the most influencing factor with regard to energy absorption. It is statistically analyzed in order to develop predictive models for the optimization of joint performance..

Ariaee et al. [10] applied RSM and Central Composite Rotatable Design (CCRD) to optimize the mechanical performance of the composite-steel single-lap joints. In their case study, curing time and temperature were the selected key factors, while the authors developed mathematical models for the prediction of the shear strength and elongation. ANOVA confirmed curing temperature was indeed the most important variable that dictates joint strength, a methodology which allowed optimizing the adhesive bonding process, and experimental validation proved the accuracy of the predicted values. Besides, Kraisornkachit et al. [11] have introduced active learning and machine learning-based multi-objective optimization approach to optimize the adhesive joint strength and elastic modulus in epoxy adhesives. Their study adopted a methodology of training the machine learning model with 32 experimental conditions, which validated the accuracy using K-fold cross-validation and

statistical analysis mainly by Bayesian optimization to study the trade-off involving adhesive strength and modulus.

Optimum failure load, production time, and mass in adhesively bonded 3D-printed single lap joints were investigated by Ozturk [12] using the RSM method. It was found that OL had the most dominant factor in failure load, and AT had a great influence on the production of time and mass. To this end, ANOVA and CCD were further carried out to optimize the performances of the joints with the least production time and utilization of materials. In a related vein, Gorgun [13] applied the BB design in addition to ANOVA in order to obtain the optimum bonding conditions for thermoplastic adhesive joints. The study examined variables such as the mixing ratio, curing time, and primer application, and obtained a quadratic model that can make an accurate prediction of bond performance. Validity was further supported by the high values of the R-squared and the significant F-values..

Sutherland et al. [14] utilized statistical experimental design procedures such as ANOVA to determine the strength of adhesively bonded T-joints commonly used in marine composite structures. They studied the influence of the level of surface preparation, cleaning methods, and types of adhesives on joint strength. The statistical analysis showed that there were large interactions among these factors. The complex relationships of the factors in interaction plots were presented in a useful way, enabling the derivation of practical recommendations for real adhesive joint optimization in marine applications. Finally, the work by Haddou et al. [15], applied full factorial DOE to optimize the strength of notched single-lap adhesive joints. The authors documented that the adhesive thickness was the most influential factor on joint strength with the largest contribution ratio of 58.81% to its overall performance. The notch depth and extension also played an important role, and a quadratic regression model was developed to predict the optimum joint strength.

Cetin and Fossi [16] introduced the optimization of hygrothermal mechanical strength of adhesively bonded 3D-printed joints with the Taguchi method, in this work, the effects of surface patterns, adhesive types, and aging durations on lap shear strength were evaluated with a Taguchi L16 orthogonal array. From the ANOVA analysis, adhesive type was found as the most effective factor with 60.76%, followed by the aging duration factor with 23.62%. Regression analysis confirmed the experimental results and proved that the Taguchi method was efficient in optimizing adhesive joint performance under environmental stressors.

Analytical models play a crucial role in understanding stress distributions within the adhesive layer, with the Bigwood and Crocombe model [17] being widely recognized for its ability to predict shear and peel stresses accurately in various joint configurations. Abbasi et al. [18] investigated the effectiveness of the backface strain (BFS) method in detecting damage initiation and propagation in composite single-lap joints (SLJs). They utilized the Bigwood and Crocombe analytical model to explain the presence of the zero strain point (ZSP) on the backface of the joint and correlated the experimental findings with the analytical predictions. Their results demonstrated the capability of this model to predict stress distributions under varying adhesive types and joint dimensions. Similarly, Abbasi et al. [19] analyzed the effect of bonding area dimensions on the mechanical behavior of SLJs, employing the Bigwood and Crocombe model to estimate shear and peel stress distributions. Their findings highlighted the model's utility in assessing the influence of joint width, overlap length, and adherend thickness on load capacity and failure mechanisms. Goglio et al. [20] conducted an experimental study on the impact rupture of adhesively bonded joints under different stress combinations, incorporating the Bigwood and Crocombe model to evaluate the shear and peel stresses under dynamic loading conditions. Their work demonstrated the model's robustness in predicting failure under combined loading scenarios.

Weißgraeber et al. [21] proposed a general sandwich-type analytical model for adhesive joints with composite adherends, extending the Bigwood and Crocombe model by

incorporating First Order Shear Deformation Theory (FSDT) to account for shear deformations in fiber-reinforced plastic (FRP) adherends. Their study provided a more comprehensive understanding of stress distributions in various joint configurations. Domínguez et al. [22] focused on hybrid joints between fiber-reinforced plastic (FRP) and steel panels reinforced with tubular structures. They applied the Bigwood and Crocombe model to estimate interlaminar stresses and validate the analytical predictions against finite element analysis (FEA) results. Momm and Fleming [23] employed the Bigwood and Crocombe model to investigate adhesive degradation effects in real-life bonded joints exposed to environmental conditions. Their study incorporated adhesive plasticity and aging effects into the model, providing a comprehensive approach to stress analysis under non-pristine conditions. Methfessel and Becker [24] applied the Bigwood and Crocombe model in a higher-order displacement approach for thick adhesive joints. The model was used to estimate stress distributions across the adhesive thickness, showing improved accuracy compared to traditional thin-layer assumptions. Wang et al. [25] adopted the Bigwood and Crocombe model to analyze adhesive joint strength with adherend yielding effects. They modified the model to accommodate nonlinear adherend behavior, allowing for better predictions of joint performance under high-load conditions.

da Silva et al. [26] compared elastic and nonlinear adhesives using the Bigwood and Crocombe model. The research demonstrated that the model could be extended to nonlinear adhesives and effectively capture the impact of different adhesive thicknesses on stress distribution. Additionally, the study assessed the computational efficiency of the model, highlighting its advantages in terms of preparation and solution time compared to more complex numerical methods. In another study, da Silva et al. [27] conducted a comprehensive review of analytical models for adhesively bonded joints, with a particular focus on the Bigwood and Crocombe model. The study evaluated the model's applicability under various adhesive types and loading conditions. The Bigwood and Crocombe model was found to be effective in predicting stress distributions by considering the combined effects of axial loads and bending moments. The study provided valuable insights into the practical application of the model in the design process of adhesive joints.

This study makes a significant contribution by integrating the Bigwood and Crocombe analytical model with Response Surface Methodology (RSM) to optimize the performance of double-L-bracket adhesive joints, specifically by minimizing shear and peel stresses. While extensive research has been conducted on stress distribution in adhesive joints, the novelty of this work lies in the application of RSM alongside an analytical model tailored to this specific joint configuration. This study presents a comprehensive regression model that not only predicts stress responses but also identifies optimal design configurations by systematically analyzing key parameters, including joint height, vertical and horizontal arm lengths, adhesive thickness, and applied loads. RSM provides a robust framework for simultaneously evaluating multiple design factors and developing quadratic regression models, which effectively capture the interactions between these parameters in influencing shear and peel stresses. Notably, the methodology highlights horizontal arm length as the most critical factor affecting joint performance, offering practical design guidelines that engineers can adopt to enhance structural integrity. The proposed optimization approach has been validated through a strong correlation between RSM predictions and analytical calculations, reinforcing its reliability and practical applicability.

Beyond enhancing joint performance, the proposed approach delivers substantial industrial benefits by providing a systematic method to optimize material usage, reduce production costs, and extend the service life of bonded structures under varying environmental conditions. This study supports the development of lightweight, high-strength adhesive structures that align with the growing industry demands for sustainability and efficiency in manufacturing processes. Furthermore, the insights gained from this research can be directly

implemented in real-world applications, empowering engineers to make informed decisions in design and production, ultimately resulting in safer and more reliable engineering solutions across various sectors, including aerospace, automotive, and civil engineering.

2. PROBLEM DEFINITION

The objective of this study is to optimize the design parameters of a double-L-bracket joint through an analytical approach, with a particular focus on minimizing the joint's shear and peel stresses. The shear and peel stress values were calculated using the CalcBond software [28], which employs the Bigwood-Crocombe analytical model to determine stress distributions through theoretical formulations. Providing an efficient computational framework, CalcBond facilitates accurate predictions by considering key parameters such as adhesive thickness, material properties, and loading conditions. Its capability to generate detailed stress distribution profiles enables a comprehensive understanding of joint behavior, significantly contributing to the optimization process and allowing for further analysis of the effects of various design parameters on joint performance [28]. By leveraging the Response Surface Methodology (RSM), the effects of various geometric parameters and loading conditions on the stress distribution in the joint are thoroughly investigated.

Figure 1 provides a detailed schematic of the double-L-bracket joint configuration used in this study. The total height of the joint (H) is defined as the distance from the bottom of the vertical arm to the top of the horizontal arm, and is varied between 70 mm, 80 mm, and 90 mm. The lengths of the vertical arm (L1) and the horizontal arm (L2) are also varied, with each parameter taking values of 10 mm, 20 mm, and 30 mm. The thickness of the adhesive layer (Tg) between the two brackets is another critical parameter, with values of 0.1 mm, 0.2 mm, and 0.3 mm analyzed. The forces applied to the lower arm—namely the shear force (Fx) and the peel force (Fz)—are varied at 50 N, 75 N, and 100 N. The upper arm of the joint remains fixed, while these forces are applied to the lower arm to simulate realistic loading conditions.

Table 1 outlines the mechanical properties of the materials used in the joint. The adherends are made of aluminum with a thickness of 3 mm, an elastic modulus of 70 GPa, and a Poisson's ratio of 0.3. The adhesive used to bond the brackets is Araldite 2014-2, which has an elastic modulus of 3200 MPa, a shear modulus of 0.56 GPa, and a Poisson's ratio of 0.32.

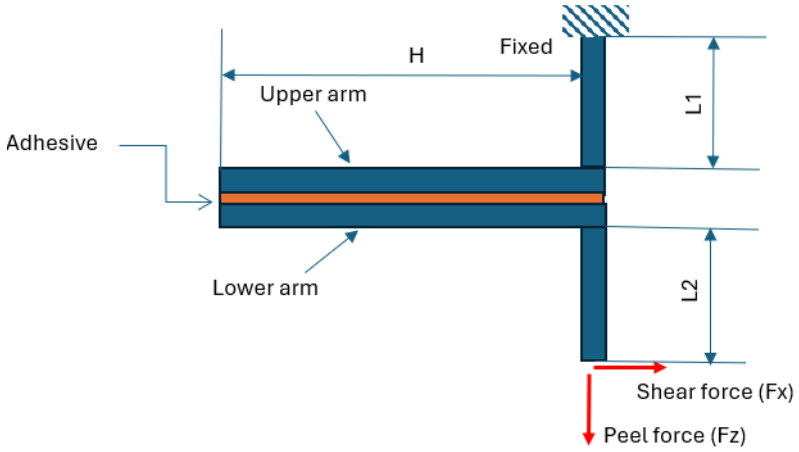

Figure 1. The configuration of double-L-bracket joint

Table 1. Mechanical properties [29, 30]

	Unit	Adherend	Adhesive
		Aluminum	Araldite 2014-2
Elastic modulus (E, GPa)	GPa	70	3.2
Shear Modulus (G_a)	GPa	25	0.56
Poisson's ratio (ν .-)	-	0.3	0.32

3. RESPONSE SURFACE METHODOLOGY (RSM) DESIGN

In the context of this study, Response Surface Methodology (RSM) is employed as a powerful statistical and mathematical tool to optimize the design parameters of a double-L-bracket joint. The primary objective is to identify the optimal combination of design variables that minimize both shear and peel stresses, which are critical failure modes in adhesive joints. To systematically investigate the effects of various design parameters on stress responses, a Box-Behnken Design (BBD) is selected as the experimental design framework. BBD is a popular form of RSM, specifically chosen for its efficiency in exploring quadratic response surfaces. It provides an effective means of conducting experiments or simulations when the aim is to build a second-order polynomial model. Unlike other design methods such as central composite design (CCD), BBD does not require experiments to be run at extreme levels (corners) of the design space, which makes it particularly suitable for cases where such conditions may be impractical or unsafe.

The design includes 54 experimental runs (Table 2), each experimental run corresponds to a specific combination of the six factors, and for each run, the shear and peel stresses are calculated using the Bigwood Crocombe analytical model. These calculated stresses are then used as response variables in the subsequent regression analysis, which aims to develop a predictive model for both shear and peel stresses. For example, in Run 7, a configuration with H = 80 mm, L1 = 30 mm, L2 = 30 mm, Tg = 0.2 mm, Fx = 100 N, and Fz = 75 N results in a shear stress of 13.4 MPa and a peel stress of 2.7 MPa.

Table 2. Design of Experiments (DOE) for Shear and Peel Stress Evaluation

DOE	H	L1	L2	Adhesive thickness	Fx	Fz	Shear stress	Peel stress
1	80	10	20	0.2	50	50	4.5	1.6
2	80	20	10	0.1	75	50	5.0	2.5
3	90	30	20	0.3	75	75	5.5	2.1
4	80	10	30	0.2	50	75	6.7	2
5	70	30	20	0.1	75	75	9.6	3
6	90	10	20	0.3	75	75	5.5	2.1
7	80	30	30	0.2	100	75	13.4	2.7
8	80	10	10	0.2	50	75	2.3	2.1
9	80	30	10	0.2	50	75	2.3	2.1
10	70	20	20	0.3	100	75	7.3	2.4
11	70	10	20	0.3	75	75	5.5	2.1
12	90	20	30	0.2	75	100	10.1	2.8
13	70	20	10	0.2	75	100	3.5	2.8
14	80	20	30	0.1	75	50	14.3	2.4
15	90	20	30	0.2	75	50	10.1	1.9
16	80	20	20	0.2	75	75	6.8	2.4
17	80	10	20	0.2	50	100	4.5	2.5
18	80	30	30	0.2	50	75	6.7	2
19	80	30	10	0.2	100	75	4.7	2.7
20	70	20	20	0.1	50	75	6.4	2.5

21	80	20	20	0.2	75	75	6.8	2.4
22	80	30	20	0.2	50	100	4.5	2.5
23	90	20	20	0.3	50	75	3.7	1.8
24	70	20	10	0.2	75	50	3.5	1.9
25	80	30	20	0.2	100	50	9.0	2.3
26	70	20	30	0.2	75	50	10	1.9
27	80	20	10	0.3	75	50	2.9	1.7
28	80	10	20	0.2	100	50	9.0	2.3
29	90	20	20	0.3	100	75	7.4	2.4
30	70	20	30	0.2	75	100	10	2.8
31	80	20	20	0.2	75	75	6.8	2.4
32	80	10	20	0.2	100	100	9.0	3.2
33	80	20	30	0.3	75	100	8.2	2.5
34	80	20	20	0.2	75	75	6.8	2.4
35	70	20	20	0.1	100	75	12.8	3.4
36	90	20	10	0.2	75	100	3.5	2.8
37	80	20	20	0.2	75	75	6.8	2.4
38	80	20	30	0.3	75	50	8.2	1.7
39	90	20	10	0.2	75	50	3.5	1.9
40	80	10	10	0.2	100	75	4.7	2.7
41	80	20	10	0.3	75	100	2.9	2.5
42	70	20	20	0.3	50	75	3.7	1.8
43	80	30	20	0.2	50	50	4.5	1.6
44	90	20	20	0.1	100	75	12.9	3.5
45	70	10	20	0.1	75	75	9.6	3
46	80	20	20	0.2	75	75	6.8	2.4
47	90	20	20	0.1	50	75	6.4	2.6
48	90	10	20	0.1	75	75	9.7	3
49	70	30	20	0.3	75	75	5.5	2.1
50	80	20	10	0.1	75	100	5.0	3.6
51	90	30	20	0.1	75	75	9.7	3
52	80	20	30	0.1	75	100	14.3	3.5
53	80	10	30	0.2	100	75	13.4	2.7
54	80	30	20	0.2	100	100	9.0	3.2

The model generated from the BBD data is evaluated based on multiple statistical metrics, including R-squared, adjusted R-squared, and predicted R-squared values, as well as the significance of individual model terms (linear, interaction, and quadratic). The ANOVA (Analysis of Variance) results are also used to assess the model's overall fit and the significance of each design factor. The use of BBD in conjunction with RSM enables the identification of key design variables that have the most significant effects on shear and peel stresses. This insight allows for targeted optimization, reducing the likelihood of failure in the joint due to excessive stresses.

4. RESULTS and DISCUSSION

4.1. Analysis of Variance (ANOVA) Results for Shear and Peel Stress

4.1.1. Shear stress ANOVA

Supplementary Table 1 shows the ANOVA results for shear stress, revealing that the model explains 99.79% of the total variance in the response. This exceptionally high R^2 value demonstrates the robustness of the model in capturing the behavior of shear stress in the joint. The linear terms contribute significantly to the model, with L2 (horizontal arm length), Fx (shear

force), and adhesive thickness (Tg) standing out as the most important factors. The F-values for these terms are extremely high, particularly for L2 (6407.20), Tg (2348.24), and Fx (3060.88), indicating that these parameters have a pronounced effect on the shear stress response. The P-values for these factors are 0.000, underscoring their statistical significance in the model. In terms of interactions, the results also highlight significant two-way interactions between L2 and Tg (F = 184.75, P = 0.000) and Tg and Fx (F = 90.53, P = 0.000). These interactions suggest that while increasing L2 raises the shear stress, the effect can be moderated by increasing adhesive thickness, which distributes the stress more effectively. Similarly, the interaction between Tg and Fx shows that a thicker adhesive layer reduces the stress concentrations caused by higher shear forces. These interaction effects emphasize the complex, non-linear relationships between design parameters and stress responses in the joint. The lack-of-fit test indicates no significant lack of fit (P = 0.21), confirming that the model accurately represents the data and does not miss any critical trends. The small error term (0.21%) further enhances confidence in the model's predictive capability.

4.1.2 Peel Stress ANOVA

Supplementary Table 2 presents the ANOVA results for peel stress, showing that the model explains 99.83% of the total variance. Similar to the shear stress model, the peel stress model exhibits a high level of statistical reliability, with an R^2 value indicating that nearly all of the variability in peel stress is captured by the model. The linear effects of Fz (peel force), Tg (adhesive thickness), and L2 (horizontal arm length) are the most significant contributors to the peel stress response. The F-values for Fz (5825.93), Tg (5616.00), and L2 (7.70) indicate the strength of their influence on peel stress, with P-values of 0.000, affirming their importance. Peel force (Fz) is the dominant factor in the model, as expected, given that peel stress directly arises from forces applied perpendicular to the adhesive bond. The large F-value and corresponding low P-value underscore that any increase in Fz leads to a substantial rise in peel stress. The adhesive thickness (Tg) also plays a critical role, with a large negative coefficient indicating that increasing the thickness of the adhesive layer effectively reduces peel stress by distributing the applied forces more evenly. The interaction effects for peel stress, while not as pronounced as those for shear stress, still show significant relationships. For example, the interaction between L2 and Tg (F = 5.78, P = 0.024) demonstrates that reducing horizontal arm length can help mitigate peel stress, particularly when combined with a thicker adhesive layer. Moreover, the interaction between Tg and Fx (F = 52.00, P = 0.000) suggests that a thicker adhesive layer can offset the increase in peel stress caused by higher shear forces, although the primary influence on peel stress remains Fz. The model also passes the lack-of-fit test (P = 0.17), confirming that it provides an accurate fit to the experimental data. The residual error is minimal, accounting for only 0.17% of the total variation, further supporting the model's reliability in predicting peel stress in double-L-bracket joints.

4.2. Regression Models for Shear and Peel Stress

4.2.1. Shear Stress Regression Model

The regression model for shear stress was developed using Response Surface Methodology (RSM), with six factors (H, L1, L2, Tg, Fx, Fz) included as predictors. The model was constructed to predict the shear stress response as a function of these parameters, and its statistical performance was evaluated through various metrics, including the significance of individual terms, model fit, and residual analysis. The regression equation for shear stress is provided in the supplementary document as Eq. (1).

The coded coefficients from the regression model, presented in Supplementary Table 3, highlight the key factors influencing shear stress. Notably, the most significant term is the horizontal arm length (L2), with a large positive coefficient (3.4000) and a highly significant T-value (80.04). This indicates that increasing L2 has a strong positive effect on shear stress. Physically, this can be explained by the fact that a longer horizontal arm amplifies the moment arm for the applied forces, increasing the torque and thus the shear stress at the adhesive interface. This result is consistent with mechanical theory and reinforces the importance of carefully controlling L2 to prevent excessive shear forces in the joint.

Adhesive thickness (Tg) also plays a critical role in the model, with a substantial negative coefficient (-2.0583) and a T-value of -48.46. This negative sign indicates that increasing Tg reduces shear stress, which is a reflection of the adhesive's ability to absorb and distribute the applied forces more effectively as its thickness increases. A thicker adhesive layer allows for more elastic deformation, spreading the shear load over a larger area and reducing peak stress concentrations. This finding aligns with expectations from adhesive joint theory, where thicker bond lines are often associated with improved stress distribution and lower localized stresses.

The applied shear force (Fx) is another significant factor, with a positive coefficient (2.3500) and a T-value of 55.33. As expected, increasing Fx directly raises the shear stress in the joint, as the magnitude of the applied force determines the load borne by the adhesive layer. This result is particularly important for design applications where shear forces cannot be easily reduced, emphasizing the need for compensatory design strategies, such as increasing Tg or reducing L2, to offset the rise in stress caused by high shear forces.

In addition to the main effects, the regression model also includes interaction and quadratic terms to capture more complex relationships between the factors. For example, the interaction between L2 and Tg, with a coefficient of -1.0000 and a T-value of -13.59, indicates that the effect of L2 on shear stress is moderated by the adhesive thickness. This interaction suggests that while increasing L2 raises the shear stress, this effect is less pronounced when Tg is large. In other words, the detrimental impact of long horizontal arms can be mitigated by using thicker adhesive layers, which helps distribute the shear forces more evenly.

Table 3. Model Summary: Shear Stress and Peel Stress Regression Statistics

Shear stress						
S	**R-sq**	**R-sq(adj)**	**PRESS**	**R-sq(pred)**	**AICc**	**BIC**
0.208090	99.79%	99.58%	5.88190	98.92%	74.74	59.92
Peel stress						
S	**R-sq**	**R-sq(adj)**	**PRESS**	**R-sq(pred)**	**AICc**	**BIC**
0.0294174	99.83%	99.66%	0.117551	99.12%	-136.55	-151.37

Table 3 presents the model summary. The model fit is excellent, with an R-squared value of 99.79%, indicating that nearly all the variability in shear stress is explained by the model. The adjusted R-squared (99.58%) and predicted R-squared (98.92%) are similarly high, confirming that the model performs well both in fitting the training data and predicting new, unseen data. The low standard error (S = 0.208090) and the results from the analysis of variance (ANOVA) further support the model's reliability.

4.2.2. Peel Stress Regression Model

Similar to the shear stress model, the peel stress regression model was developed using RSM and incorporates the same six factors (H, L1, L2, Tg, Fx, Fz). Peel stress, which arises when forces act perpendicular to the adhesive layer, is a key factor in joint failure modes, as adhesive bonds are typically weaker in tension than in shear. Thus, understanding the factors that

influence peel stress is critical for designing robust joints. The regression equation for shear stress is provided in the supplementary document as Eq. (2).

Supplementary Table 4 presents the coded coefficients for the peel stress regression model, with the peel force (Fz) emerging as the most significant factor. The coefficient for Fz is positive (0.45833) and highly significant (T-value of 76.33), indicating that increasing Fz directly raises peel stress. This result is consistent with the physics of peel stress, where forces applied perpendicular to the bond line concentrate stress at the edges of the adhesive layer, making the joint susceptible to peeling or delamination. The strong influence of Fz suggests that minimizing peel forces in applications where peeling is a concern should be a primary design objective.

Adhesive thickness (Tg) also plays a critical role in the peel stress model, with a large negative coefficient (-0.45000) and a highly significant T-value (-74.94). As in the shear stress model, increasing Tg reduces peel stress by allowing the adhesive to better absorb and distribute the applied forces. Thicker adhesive layers reduce the concentration of peel stresses at the edges of the bond line, where failures are most likely to initiate. This finding underscores the importance of optimizing Tg in applications where peel forces are expected, as it provides a straightforward method for reducing stress and enhancing joint durability. Interestingly, the horizontal arm length (L2) has a smaller, but still significant, negative effect on peel stress, with a coefficient of -0.01667 and a T-value of -2.78. This indicates that reducing L2 can help mitigate peel stress, although its impact is less pronounced than Tg or Fz. The physical interpretation of this result is that shorter horizontal arms reduce the leverage applied to the adhesive bond, thereby decreasing the tendency for the joint to peel under applied forces.

Quadratic terms and interactions are also included in the model to capture non-linear effects and the combined influence of multiple parameters. For example, the interaction between Tg and Fx has a significant negative coefficient (-0.0750), indicating that the effect of Fx on peel stress is moderated by the adhesive thickness. When Tg is large, the peel stress induced by Fx is less severe, reflecting the adhesive's improved ability to distribute the applied forces across a thicker bond line. This interaction highlights the complex nature of peel stress in multi-parameter systems and the need for a holistic approach to joint design.

The peel stress model also shows an excellent fit to the data (Table 3), with an R-squared value of 99.83% and similarly high adjusted and predicted R-squared values (99.66% and 99.12%, respectively). The low standard error (S = 0.0294174) indicates that the model provides precise predictions of peel stress, while the results from the ANOVA confirm the statistical significance of the model as a whole.

The high significance of most terms in the model, as reflected by their low P-values and high T-values, indicates that the relationships between the input factors and peel stress are well-captured by the regression model. The model can be used to accurately predict peel stress under a wide range of joint configurations and offers valuable insights into the design strategies that can be employed to minimize peel stress.

4.3. Graphical Analysis and Visualization of Stress Responses

4.3.1. Residual Analysis

Residual analysis is a fundamental tool in statistical modeling, used to validate the accuracy and reliability of regression models. The residuals represent the differences between observed values and the predicted values from the model. Proper residual analysis ensures that the model is unbiased, and it helps detect any systematic errors or patterns that may indicate a misfit.

In Figure 2 (a), the residual plot for shear stress shows a random distribution of residuals around zero, which is a key indicator that the regression model provides an unbiased and accurate prediction of the data. This randomness suggests that no patterns are present in the residuals, meaning that the model has successfully captured the relationship between the input parameters and the shear stress response. The absence of any clear trend, such as a funnel-shaped distribution or clustering of points, further indicates that the model does not suffer from heteroscedasticity, where the variance of the residuals would depend on the magnitude of the predicted values. This is critical for the validity of the model, as heteroscedasticity can lead to biased estimates and affect the confidence intervals of the regression coefficients. Additionally, the spread of the residuals in Figure 2 (a) appears consistent across the range of predicted shear stress values, supporting the assumption of homoscedasticity. Homoscedasticity implies that the variance of the residuals is constant, reinforcing the reliability of the regression model. This property ensures that the model is equally effective in predicting shear stress across both lower and higher ranges, thereby improving the generalizability of the findings.

Similarly, the residual plot for peel stress in Figure 2 (b) displays a random scatter of residuals around zero, further validating the model's predictive accuracy for peel stress. The plot shows no discernible patterns or trends, confirming that the regression model is well-suited for predicting peel stress under varying configurations. The consistency in the spread of residuals also indicates that the model handles both small and large peel stress values equally well, with no indication of bias or distortion.

Residual analysis also aids in identifying potential outliers or influential data points that may disproportionately affect the regression model. In this study, there are no significant outliers present in either the shear or peel stress residual plots, further enhancing confidence in the robustness of the model. The lack of unusual residuals suggests that the dataset is well-behaved, and that the regression models are not unduly influenced by any extreme or erroneous observations. This conclusion is critical, as outliers can distort the regression coefficients and lead to incorrect conclusions.

Overall, the residual analysis confirms that the models for both shear and peel stress are reliable, unbiased, and appropriate for the given dataset. The lack of heteroscedasticity, combined with the random distribution of residuals, reinforces the statistical soundness of the regression models and supports their use for stress prediction in the double-L-bracket joint design.

4.3.2. Pareto Charts of Standardized Effects

Pareto charts are an essential graphical tool for identifying the most influential factors in a regression model. By ranking the standardized effects of each factor, these charts provide a clear visualization of the relative importance of each design parameter in affecting the response variable. In this study, the Pareto charts for shear and peel stress highlight the key factors driving stress concentrations in the double-L-bracket joint.

Figure 3 (a) presents the Pareto chart for shear stress, which clearly demonstrates that the horizontal arm length (L2), adhesive thickness (Tg), and shear force (Fx) are the most significant contributors to shear stress. The bar corresponding to L2 is the tallest, indicating that it has the largest standardized effect on shear stress. This result is consistent with the theoretical expectation that longer horizontal arms increase the moment arm, thereby amplifying the shear forces acting on the adhesive layer. The high significance of L2 in the model underscores the need for careful control of this parameter in joint design to prevent excessive shear stress concentrations. The next most significant factor is adhesive thickness (Tg), which has a substantial negative effect on shear stress. The negative coefficient indicates that increasing Tg reduces shear stress, likely due to the adhesive's ability to absorb and distribute forces more effectively as its thickness increases. This finding reinforces the role of adhesive thickness as a

key parameter in mitigating stress and improving the joint's load-bearing capacity. The Pareto chart shows that, while L2 increases stress, Tg can counteract this effect by providing better stress distribution. The shear force (Fx) also has a major positive influence on shear stress, as expected. The higher the applied shear force, the greater the stress acting on the adhesive layer. This result emphasizes the importance of limiting Fx in applications where high shear stress is a concern. The Pareto chart indicates that the interaction between Fx and L2 should be closely monitored, as these two factors together can lead to critical stress concentrations if not properly managed. The smaller bars on the Pareto chart, representing parameters such as joint height (H), vertical arm length (L1), and peel force (Fz), indicate that these factors have relatively minor impacts on shear stress. However, it is important to note that while their individual effects may be small, their interactions with more significant factors (such as L2 and Tg) could still play a role in stress distribution. Understanding these interactions is critical for optimizing the overall joint performance.

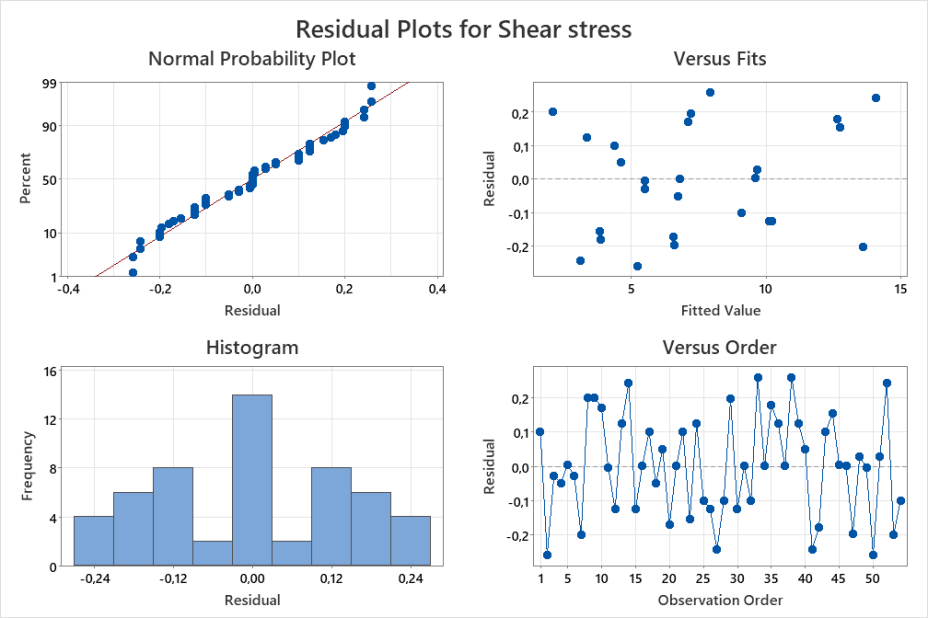

(a)

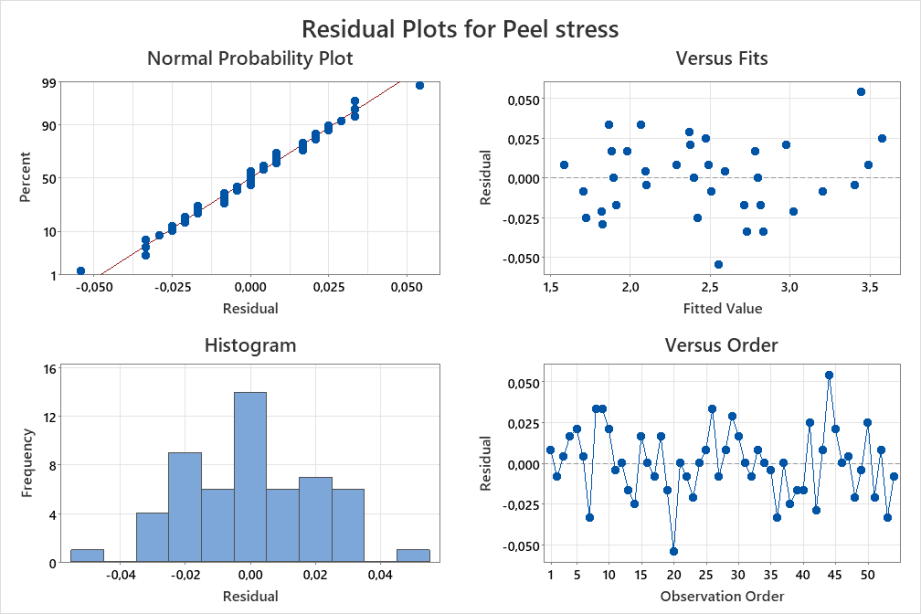

(b)

Figure 2. Residual Plots for (a) Shear and (b) Peel stress

In Figure 3 (b), the Pareto chart for peel stress highlights the dominant role of peel force (Fz) and adhesive thickness (Tg). The tallest bar corresponds to Fz, confirming that peel force is the most significant driver of peel stress. This is consistent with the physical nature of peel stress, which is directly induced by forces acting perpendicular to the adhesive layer. The high importance of Fz suggests that managing peel forces is critical for minimizing stress concentrations and preventing adhesive failure. Adhesive thickness (Tg) again emerges as a key factor, with a significant negative effect on peel stress. The negative coefficient indicates that increasing Tg reduces peel stress, likely by allowing the adhesive to better distribute the applied forces and reduce peak stress concentrations at the edges of the joint. This finding is consistent with the contour and surface plots, which show that Tg plays a crucial role in stress mitigation for both shear and peel forces. The horizontal arm length (L2) also has a notable, though smaller, negative effect on peel stress. This result suggests that reducing L2 can help to mitigate peel

stress, which may be beneficial in certain applications. However, the primary focus for controlling peel stress should be on managing Fz and optimizing Tg, as these are the most significant factors driving the stress response.

Overall, the Pareto charts provide valuable insights into the relative importance of different design parameters in influencing shear and peel stresses. The charts make it clear that L2, Tg, and Fx are the primary factors for controlling shear stress, while Fz and Tg dominate the peel stress response. These findings inform the optimization process by identifying the key parameters that should be targeted for stress minimization, offering practical guidance for improving joint design.

4.4.Visualization of Interaction Effects

4.4.1. Contour Plots for Shear and Peel Stress

Contour plots are a crucial tool in visualizing the relationship between two input parameters and their combined effect on a response variable, in this case, shear and peel stress. By holding other factors constant, these plots provide insight into how variations in specific parameter pairs influence the stress distribution within the joint.

Supplementary Figure 1 (a) presents the contour plots of shear stress, illustrating the complex interplay between key design parameters such as joint height (H), horizontal arm length (L2), vertical arm length (L1), adhesive thickness (Tg), and applied forces (Fx and Fz). The contour plots provide a visual representation of shear stress distribution across various combinations of these parameters, offering critical insights into their influence on joint performance. From the plots, it is evident that shear stress is highly dependent on the horizontal arm length (L2) and adhesive thickness (Tg), as indicated by the steep gradient transitions observed in the respective contour regions. A larger L2 generally results in lower shear stress values, contributing to a more uniform stress distribution and reducing the likelihood of stress concentration near the adhesive-substrate interface. Conversely, when L2 is reduced, shear stress becomes more localized, which may lead to premature failure due to excessive stress accumulation. Additionally, the adhesive thickness (Tg) plays a crucial role in shear stress mitigation; increasing Tg tends to reduce peak stress values and distribute loads more effectively. However, beyond a certain limit, the benefits of increased adhesive thickness may plateau, emphasizing the need for an optimized balance between material usage and joint performance. Furthermore, the applied force Fx significantly influences shear stress patterns, with higher force values leading to greater shear stress magnitudes, underscoring the importance of selecting appropriate load conditions for the intended application. The contour plots also highlight interaction effects between adhesive thickness and loading parameters, which must be carefully considered during the design process to ensure optimal joint performance and durability.

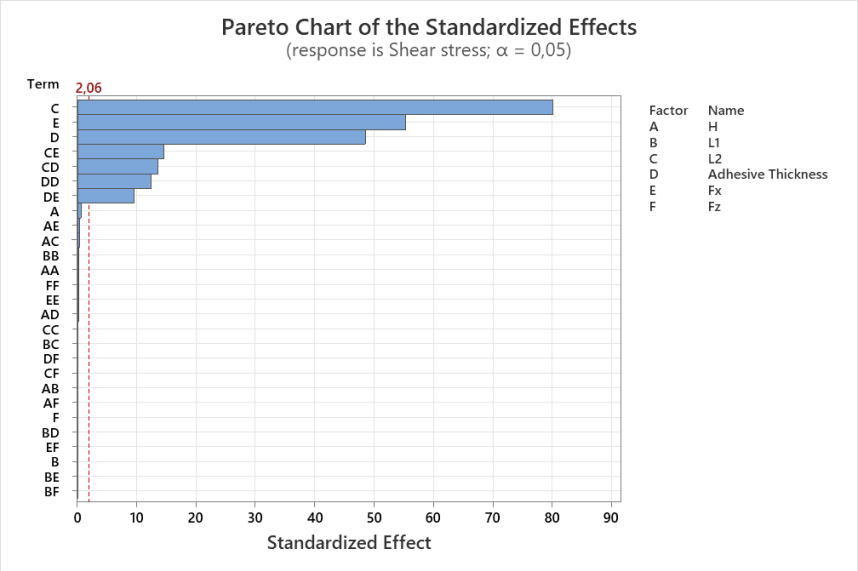

(a)

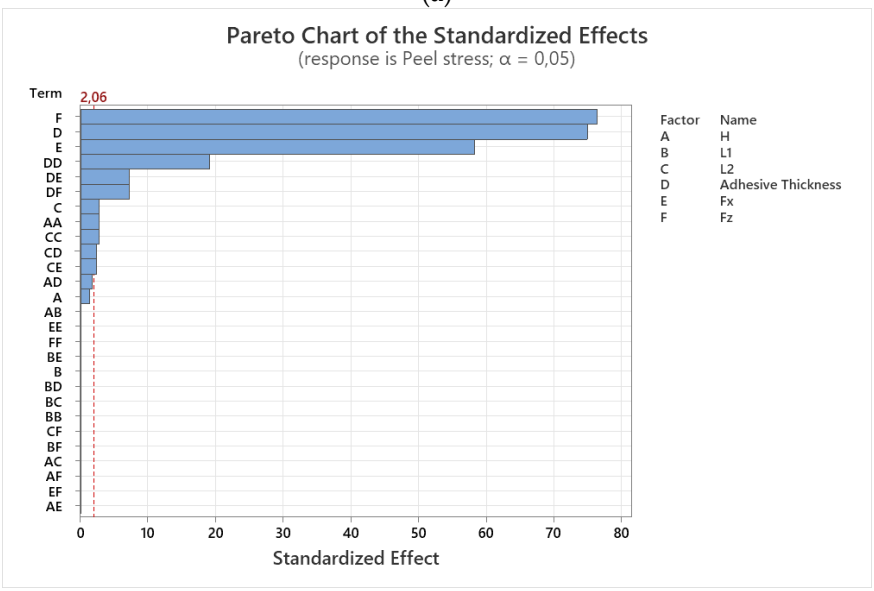

(b)

Figure 3. Pareto Chart of the Standardized Effects (a) Shear and (b) Peel stress

Supplementary Figure 1 (b) provides contour plots illustrating the distribution of peel stress in the double-L-bracket adhesive joint. Peel stress is a critical factor in bonded joints, as it contributes significantly to delamination and failure propagation at the adhesive-adherent interface. The contour plots reveal that peel stress is most influenced by vertical arm length (L1) and the applied peel force (Fz), with variations in these parameters leading to distinct stress distribution patterns. A longer L1 generally reduces peel stress concentrations, allowing for better load transfer and enhancing joint longevity. However, shorter vertical arm lengths result in higher localized peel stress, which can lead to adhesive failure under cyclic or sustained loading. Additionally, adhesive thickness (Tg) has a notable effect on peel stress distribution; increasing Tg tends to lower peel stress levels by improving the adhesive's load-bearing capability and energy absorption properties. Nevertheless, an excessively thick adhesive layer may introduce flexibility-related issues, which could adversely affect joint stiffness and load distribution efficiency. The contour plots also indicate that the interaction between peel force (Fz) and adhesive thickness (Tg) is crucial in determining the joint's overall performance, as

higher peel forces tend to exacerbate stress concentrations, especially in joints with thinner adhesive layers. The insights provided by these contour plots are invaluable in guiding the selection of optimal design parameters to minimize peel stress and extend the service life of the joint.

Overall, Supplementary Figures 1(a) and 1(b) provide a comprehensive understanding of how key design parameters influence shear and peel stress distributions in double-L-bracket adhesive joints. These visual representations facilitate the identification of critical stress regions and offer practical design recommendations for optimizing joint performance. The findings underscore the importance of selecting appropriate values for adhesive thickness, joint dimensions, and applied forces to achieve an optimal balance between structural integrity and material efficiency. By leveraging the insights gained from these contour plots, engineers can make informed design decisions to enhance joint reliability, reduce material consumption, and extend operational lifespan in applications across industries such as aerospace, automotive, and civil engineering.

4.4.2. Surface Plots for Shear and Peel Stress

While contour plots offer two-dimensional views of parameter interactions, surface plots provide a more comprehensive, three-dimensional visualization of how two factors simultaneously affect stress responses. Surface plots not only reveal the magnitude of the stresses but also depict the curvature of the response surface, providing insights into the non-linear interactions between variables.

In Figure 4(a), the surface plot for shear stress illustrates the interaction between L2 and Tg. The plot shows a pronounced increase in shear stress as L2 increases, particularly when Tg is small. The steep gradient of the surface at low Tg values indicates that small changes in L2 or Tg can lead to large changes in shear stress, especially when both parameters are at their extreme values (large L2 and thin Tg). As Tg increases, the surface flattens, indicating that the adhesive layer absorbs and distributes the applied forces more effectively, reducing the overall stress. The surface plot clearly demonstrates the non-linear relationship between L2 and Tg, with Tg acting as a critical factor in controlling shear stress under high L2 conditions. This three-dimensional visualization also highlights the diminishing returns of increasing Tg beyond a certain point. While increasing Tg significantly reduces shear stress for large L2 values, the stress reduction becomes less pronounced at very high Tg levels, suggesting an optimal adhesive thickness that balances stress mitigation and material usage. This insight is valuable for practical applications where increasing Tg too much could result in excessive material costs or manufacturing difficulties.

Figure 4b presents the surface plot for peel stress, depicting the interaction between peel force (Fz) and adhesive thickness (Tg). Similar to the shear stress surface plot, the peel stress increases steeply with increasing Fz, particularly when Tg is small. The steep slopes at low Tg values indicate that the joint is highly sensitive to peel forces when the adhesive layer is thin, leading to higher stress concentrations. As Tg increases, the surface flattens, showing that the adhesive layer is better able to distribute the peel forces, reducing the peak stresses. The surface plot also reveals the non-linear nature of the interaction between Fz and Tg. While increasing Tg significantly reduces peel stress for high Fz values, the benefits of thicker adhesive layers become less pronounced beyond a certain point. This suggests that there is an optimal Tg value, beyond which further increases in thickness do not yield substantial stress reduction. Designers must therefore carefully balance the thickness of the adhesive layer with the expected peel forces to achieve the desired performance without overusing material. Both surface plots provide critical insights into the non-linear interactions between the input parameters. They emphasize the importance of balancing the horizontal arm length (L2) and peel force (Fz) with

the adhesive thickness (Tg) to minimize both shear and peel stresses. The three-dimensional nature of these plots allows for a more nuanced understanding of how small changes in design parameters can lead to significant stress variations, offering valuable guidance for optimizing joint designs in practical applications.

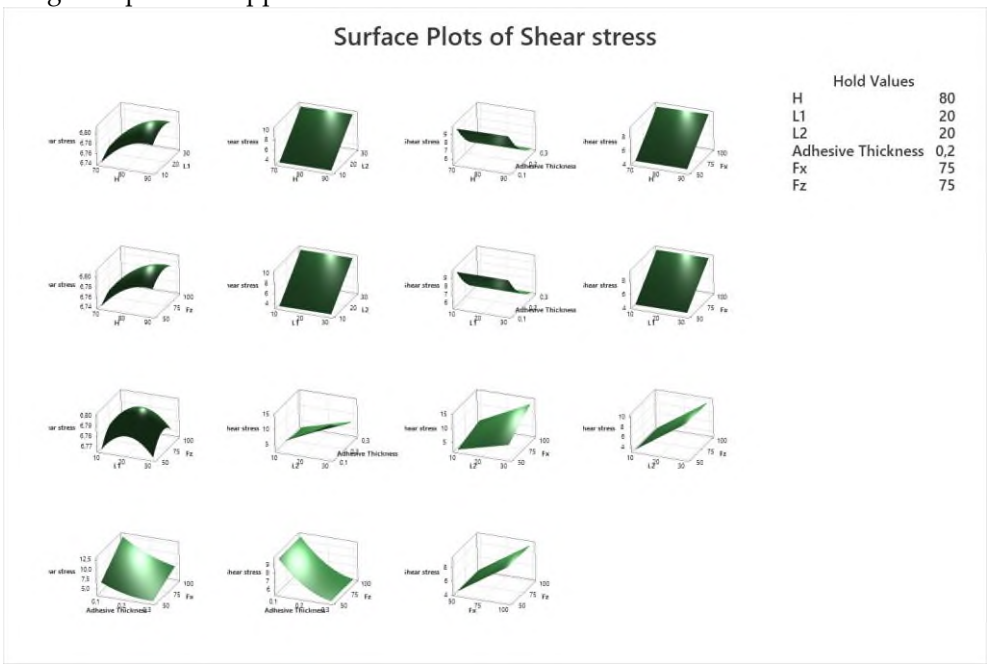

(a)

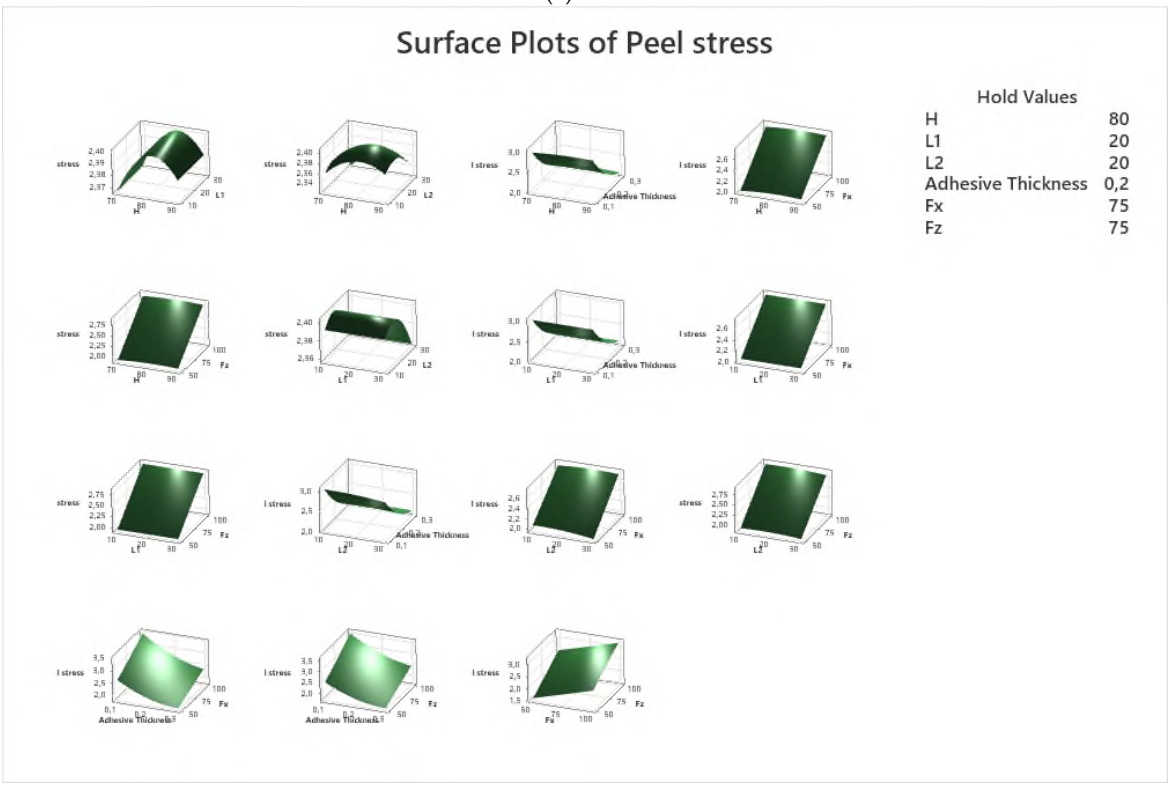

(b)

Figure 4. Surface Plots of (a) Shear and (b) Peel stress

4.5. Optimization and Interaction Effects

4.5.1 Interaction Plots for Stress Minimization

A thorough understanding of the interactions between design parameters is essential to minimize shear and peel stresses in the double-L-bracket joint. Interaction plots help visualize the combined effects of different variables on stress levels, revealing important trends that guide the optimization process.

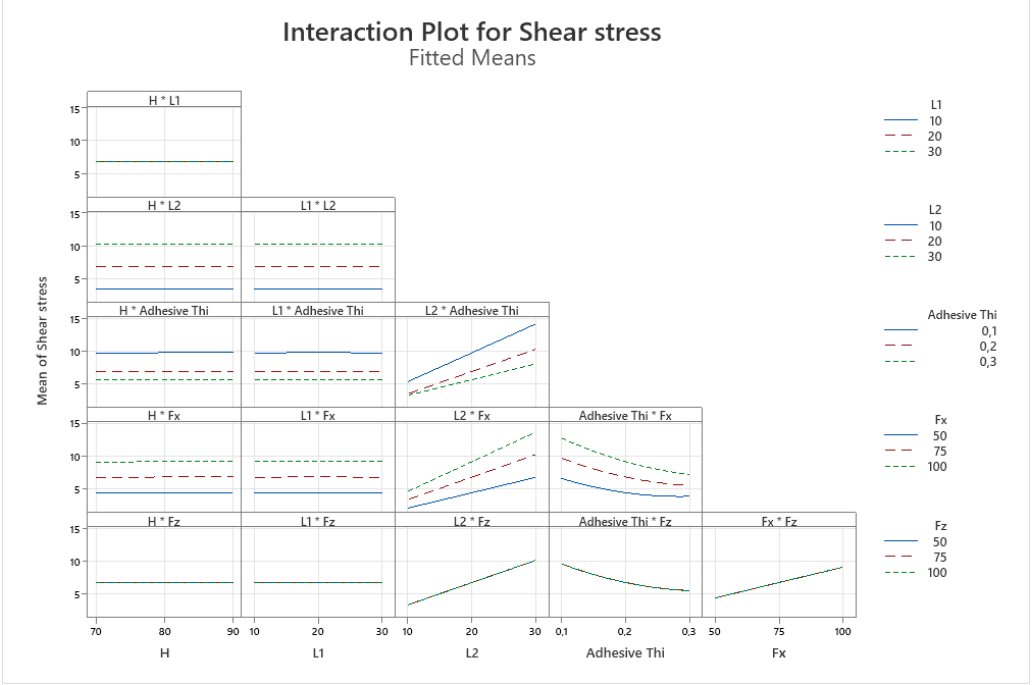

(a)

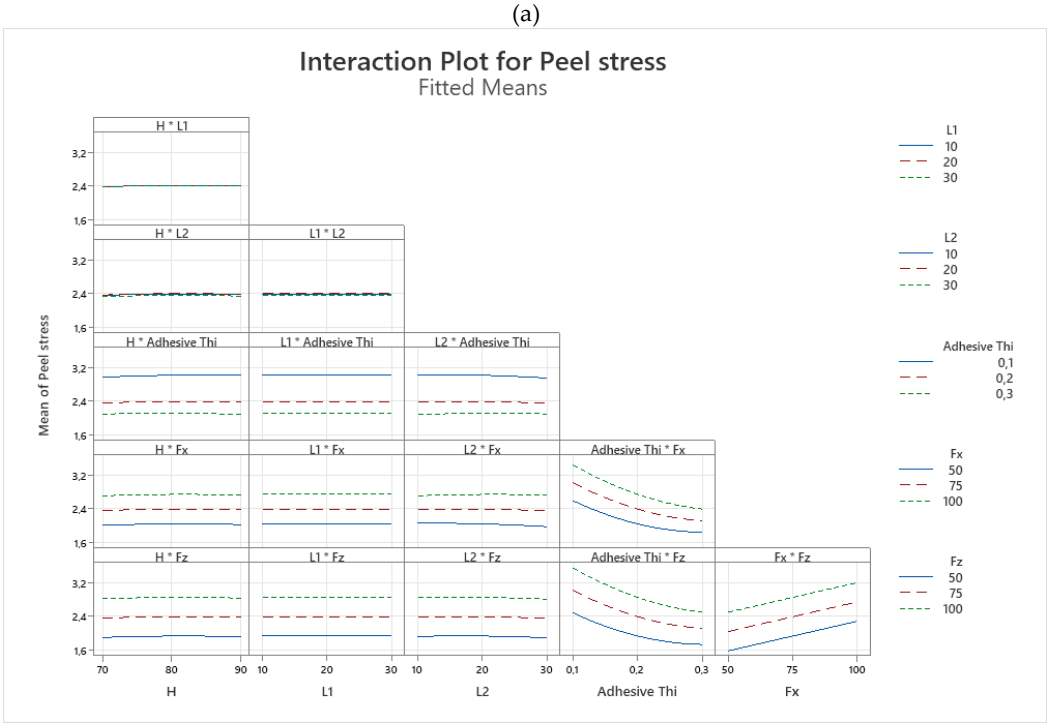

(b)

Figure 5. Interaction Plots for (a) Shear and (b) Peel stress

In Figure 5(a), the interaction between horizontal arm length (L2) and applied shear force (Fx) shows that as both parameters increase, shear stress rises significantly. This effect is expected because a longer L2 increases the moment arm for the applied force Fx, leading to greater shear forces concentrated at the adhesive interface. Simultaneously, higher Fx directly increases the stress applied to the joint. This interaction highlights the need for careful management of L2 and Fx to prevent excessive shear stress, particularly in designs requiring extended horizontal arms. However, the interaction between adhesive thickness (Tg) and Fx shows a different behavior. As Tg increases, the shear stress decreases, even with an increase in Fx. This suggests that a thicker adhesive layer improves the stress distribution, mitigating localized stress concentrations. The increased thickness allows for more elastic deformation of the adhesive, which absorbs and dissipates the applied shear forces more effectively. Therefore, Tg serves as a critical parameter to control when aiming to reduce shear stress in configurations that involve high shear forces.

The peel stress interaction plots, shown in Figure 5(b), reveal similar trends. As the peel force (Fz) increases, the peel stress increases substantially, especially when the adhesive thickness (Tg) is thin. This is due to the inability of thin adhesive layers to adequately distribute the peel forces, resulting in concentrated stresses at the edges of the joint. In contrast, increasing Tg mitigates peel stress, as the thicker adhesive layer can flex and distribute the force more evenly across the bond line. Interestingly, the interaction between joint height (H) and Fz has a less pronounced effect on peel stress. Although variations in H have a measurable impact, the dominant factor remains Fz. Therefore, the optimization of Fz and Tg is crucial for minimizing peel stress, while the height (H) plays a secondary role in the stress distribution.

These interaction plots underscore the importance of controlling the parameters that influence shear and peel stresses the most. For example, while increasing L2 and Fx exacerbates shear stress, the detrimental effects can be countered by increasing Tg. Similarly, optimizing Tg and managing Fz are critical to reducing peel stress. These findings demonstrate the complex interplay between design parameters and highlight the need for a multi-response optimization approach to ensure a balanced design.

4.5.2 Response Optimization and Comparison with Analytical Calculations

The multi-response optimization of the joint design is performed using a desirability function, which balances the minimization of both shear and peel stresses. The optimization aims to find a configuration that reduces both stresses simultaneously, while also taking into account the interactions between parameters. The results of the optimization are shown in Figure 6, which presents the optimal settings for each parameter: joint height (H) of 90 mm, vertical arm length (L1) of 30 mm, horizontal arm length (L2) of 10 mm, adhesive thickness (Tg) of 0.2616 mm, and applied forces Fx and Fz of 50 N each. The optimization yields a peel stress of 1.450 MPa and a shear stress of 2.120 MPa, both of which are significantly lower than the other configurations tested in the design of experiments. The composite desirability score of 1.000 indicates that this solution represents the optimal balance between minimizing both shear and peel stresses. Figure 6 also shows the sensitivity of each parameter to the stress responses. For instance, the steep slopes of the Fx and L2 curves indicate their strong influence on shear stress. Conversely, the Tg curve shows a more moderate, yet consistent, reduction in stress as adhesive thickness increases. The peel stress plot reveals similar sensitivities, with Tg playing a crucial role in lowering stress as its value approaches the upper limit.

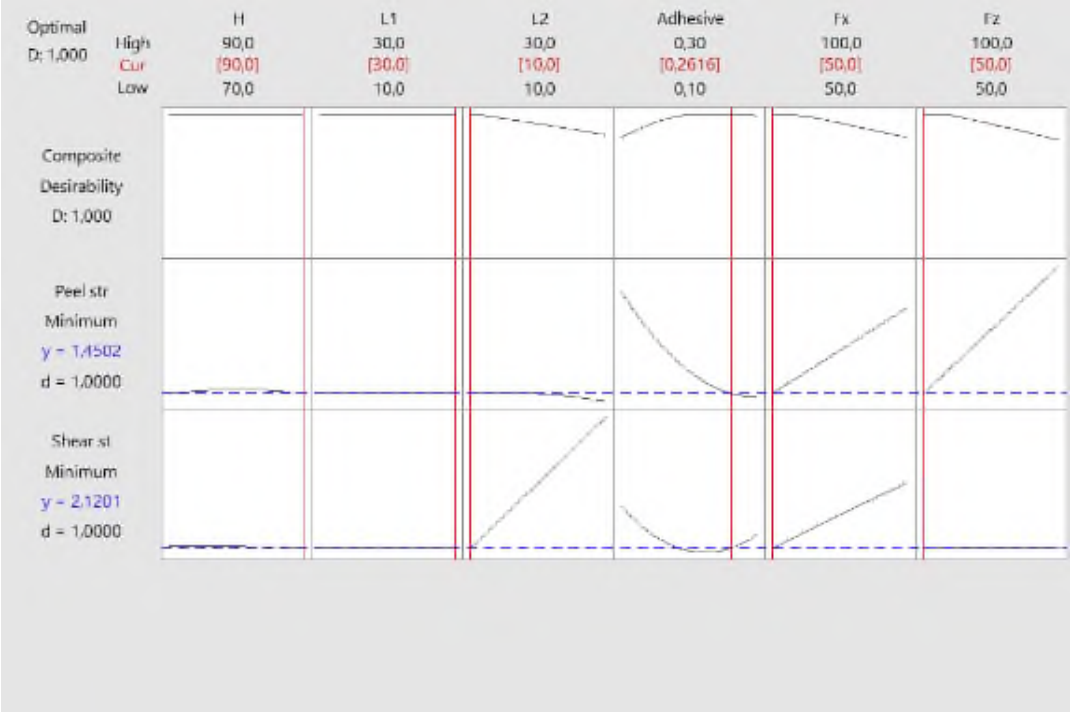

Figure 6. Optimization Plot for Shear and Peel Stress Minimization Using Composite Desirability

Table 4. Comparison of Optimized and Analytical Stress Predictions for Double-L-Bracket Joint

Variable	**Setting**			
H	90			
L1	30			
L2	10			
Adhesive Thickness	0.261616			
Fx	50			
Fz	50			
Response	**Fit**	**SE Fit**	**95% CI**	**95% PI**
Peel stress	1.4502	0.0391	(1.3698; 1.5305)	(1.3496; 1.5507)
Shear stress	2.120	0.276	(1.552; 2.688)	(1.409; 2.831)
Analytical				
Peel stress (MPa)	1.5			
Shear stress (MPa)	2.0			

A comparison of the optimized results with the analytical calculations derived from the Bigwood and Crocombe model, as shown in Table 4, validates the RSM optimization. The analytically calculated peel stress is 1.5 MPa, while the shear stress is 2.0 MPa—both values are in close agreement with the RSM-predicted results of 1.450 MPa for peel stress and 2.120 MPa for shear stress. The small discrepancies, amounting to 3.33% for peel stress and 6% for shear stress, are well within acceptable error margins for such calculations. These slight differences are attributable to the inherent approximations in the regression model used by RSM but are not significant enough to undermine the reliability of the optimization process.

The optimization also highlights the critical role of adhesive thickness in minimizing both shear and peel stresses. A Tg value of 0.2616 mm was found to be optimal, as it provides a balance between reducing stress concentrations and maintaining the adhesive's structural

integrity. Although thicker adhesive layers generally perform better at reducing stress, practical limitations such as manufacturing constraints and material costs necessitate a compromise. The selected thickness offers the best trade-off between performance and feasibility.

Another key finding from the optimization is the influence of L2 on shear stress. The optimal configuration involves reducing L2 to 10 mm, which significantly reduces the shear stress by minimizing the moment arm created by Fx. However, to maintain overall joint stability and load-bearing capacity, the optimization compensates by selecting a larger joint height (H) and vertical arm length (L1), ensuring that the design remains structurally sound. The desirability function used in this optimization process allows for a comprehensive evaluation of the trade-offs between different design objectives. The final configuration achieves the best possible balance between minimizing shear and peel stresses while taking into account practical constraints such as adhesive thickness, arm lengths, and applied forces. The composite desirability score of 1.000 confirms that this solution is optimal for the given design requirements.

In conclusion, the optimization process has successfully minimized both shear and peel stresses in the double-L-bracket joint. The close agreement between the RSM-based predictions and analytical calculations further validates the robustness of the optimization approach. The selected configuration provides a practical and efficient solution for real-world joint designs, where stress minimization is critical for ensuring long-term performance and reliability.

5. CONCLUDING REMARKS

This study successfully applied Response Surface Methodology (RSM) to optimize the shear and peel stresses in a double-L-bracket joint. By employing a Bigwood & Crocombe analytical model and using a Box-Behnken Design (BBD), the key factors affecting stress—horizontal arm length (L2), adhesive thickness (Tg), and applied forces (Fx and Fz)—were systematically analyzed. The optimization results showed that reducing L2 and increasing Tg can effectively minimize both shear and peel stresses, with the optimal configuration achieving stress levels closely aligned with analytical predictions. The findings provide valuable insights into the design of adhesive joints, offering practical guidelines for minimizing stress concentrations and improving structural durability in various engineering applications. This approach demonstrates the utility of RSM in complex joint design problems, providing a robust framework for optimizing multi-parameter systems.

Declaration of Ethical Standards

The author declares that the research was conducted in accordance with ethical standards. No human or animal subjects were involved in this study, and all ethical guidelines pertinent to the field have been followed.

Credit Authorship Contribution Statement

This work was solely conducted by Bertan Beylergil, who was responsible for the conception, design, data collection, analysis, and interpretation, as well as drafting the manuscript and approving the final version for submission.

Declaration of Competing Interest

The author declares that there are no conflicts of interest or competing interests regarding the publication of this article.

Funding / Acknowledgements

The author gratefully acknowledge financial support from the Scientific and Technological Research Council of Turkey (TÜBİTAK) with project number 218M710.

Data Availability

The author confirms that the data supporting the findings of this study are available within the article. Additional data, if required, can be provided by the author upon reasonable request.

REFERENCES

[1] R. D. Adams, Ed., *Adhesive Bonding: Science, Technology and Applications*, 2nd ed. Elsevier, 2021. doi: 10.1016/C2019-0-00395-0.

[2] L. F. M. da Silva, P. J. C. Neves, R. D. Adams, and J. K. Spelt, "Analytical models of adhesively bonded joints—Part I: Literature survey," *International Journal of Adhesion and Adhesives*, vol. 29, no. 3, pp. 319–330, 2009.

[3] C. Yildirim, H. Ulus, B. Beylergil, A. Al-Nadhari, S. Topal, and M. Yildiz, "Tailoring adherend surfaces for enhanced bonding in CF/PEKK composites: Comparative analysis of atmospheric plasma activation and conventional treatments," *Composites Part A: Applied Science and Manufacturing*, vol. 180, 2024, Art. no. 108101.

[4] L. F. M. da Silva, T. N. S. S. Rodrigues, M. A. V. Figueiredo, M. F. S. F. de Moura, and J. A. G. Chousal, "Effect of adhesive type and thickness on the lap shear strength," *The Journal of Adhesion*, vol. 82, no. 11, pp. 1091–1115, 2006.

[5] M. H. Kim, H. S. Hong, and Y. C. Kim, "Determination of failure envelope of functionally graded adhesive bonded joints by using mixed mode continuum damage model and response surface method," *International Journal of Adhesion and Adhesives*, vol. 106, 2021, Art. no. 102815.

[6] A. J. A. Vieira, R. D. S. G. Campilho, and K. Madani, "Statistical analysis of adhesive rod-tube joints under tensile stress for structural applications," *Journal of the Brazilian Society of Mechanical Sciences and Engineering*, vol. 46, no. 574, 2024.

[7] C. Mandolfino, L. Cassettari, M. Pizzorni, S. Saccaro, and E. Lertora, "A Response Surface Methodology approach to improve adhesive bonding of pulsed laser treated CFRP composites," *Polymers*, vol. 15, no. 1, 2023, Art. no. 121.

[8] J. M. Arenas, J. J. Narbon, and C. Alia, "Optimum adhesive thickness in structural adhesive joints using statistical techniques based on Weibull distribution," *International Journal of Adhesion and Adhesives*, vol. 31, no. 4, pp. 265–270, 2010.

[9] Y. Wang and K. Zeng, "Parameter optimization of particle-reinforced adhesive bonded joints based on the response surface method," *Journal of Adhesion Science and Technology*, vol. 37, no. 8, pp. 1311–1325, 2023.

[10] S. Ariaee, A. Tutunchi, A. Kianvash, and A. A. Entezami, "Modeling and optimization of mechanical behavior of bonded composite–steel single lap joints by response surface methodology," *International Journal of Adhesion and Adhesives*, vol. 54, pp. 30–39, 2014.

[11] P. Kraisornkachit, M. Naito, C. Kang, and C. Sato, "Multi-objective optimization of adhesive joint strength and elastic modulus of adhesive epoxy with active learning," *Materials*, vol. 17, no. 12, 2024, Art. no. 2866.

[12] F. H. Öztürk, "Optimization of adherend thickness and overlap length on failure load of bonded 3D printed PETG parts using response surface method," *Rapid Prototyping Journal*, vol. 30, no. 8, pp. 1579–1591, 2024.

[13] E. Gorgun, "Ultrasonic testing and surface conditioning techniques for enhanced thermoplastic adhesive bonds," *Journal of Mechanical Science and Technology*, vol. 38, no. 3, pp. 1227–1236, 2024.

[14] L. S. Sutherland, C. Amado, and C. Guedes Soares, "Statistical experimental design techniques to investigate the strength of adhesively bonded T-joints," *Composite Structures*, vol. 159, pp. 445–454, 2017.

[15] Y. M. Haddou, M. Salem, A. Amiri, R. Amiri, and S. Abid, "Numerical analysis and optimization of adhesively-bonded single lap joints by adherend notching using a full factorial design of experiment," *International Journal of Adhesion and Adhesives*, vol. 126, 2023, Art. no. 103482.

[16] E. Cetin and C. T. Fossi, "Experimental investigation on mechanical strength of adhesively bonded 3D-printed joints under hygrothermal conditions using Taguchi method," *International Journal of Adhesion and Adhesives*, vol. 126, 2023, Art. no. 103472.

[17] A. D. Crocombe and D. A. Bigwood, "Non-linear adhesive bonded joint design analyses," *International Journal of Adhesion and Adhesives.*, vol. 10, pp. 31–41, 1990.

[18] M. Abbasi, R. Ciardiello, and L. Goglio, "Backface strain as an index to detect damage initiation in composite single-lap bonded joints: Effects of adhesive type and joint dimensions," *International Journal of Adhesion and Adhesives*, vol. 134, 2024, Art. no. 103791.

[19] M. Abbasi, R. Ciardiello, and L. Goglio, "Experimental study on the effect of bonding area dimensions on the mechanical behavior of composite single-lap joint with epoxy and polyurethane adhesives," *Applied Sciences*, vol. 13, no. 7683, 2023.

[20] L. Goglio and M. Rossetto, "Impact rupture of structural adhesive joints under different stress combinations," *International Journal of Impact Engineering*, vol. 35, pp. 635–643, 2008.

[21] P. Weißgraeber, N. Stein, and W. Becker, "A general sandwich-type model for adhesive joints with composite adherends," *International Journal of Adhesion and Adhesives*, vol. 55, pp. 56–63, 2014.

[22] F. Domínguez and L. Carral, "The hybrid joints between an FRP panel and a steel panel through tubular reinforcements: A methodology for interlaminar stress calculations," *Applied Sciences*, vol. 10, no. 3962, 2020.

[23] G. G. Momm and D. Fleming, "Analytical models for stress analysis of real-life bonded joints," *The Journal of Adhesion*, vol. 98, no. 14, pp. 2253–2276, 2022.

[24] T. S. Methfessel and W. Becker, "A generalized model for predicting stress distributions in thick adhesive joints using a higher-order displacement approach," *Composite Structures*, vol. 291, 2022, Art. no. 115556.

[25] R. X. Wang, J. Cui, A. N. Sinclair, and J. K. Spelt, "Strength of adhesive joints with adherend yielding: I. Analytical model," *The Journal of Adhesion*, vol. 79, no. 1, pp. 23–48, 2003.

[26] L. F. M. da Silva, P. J. C. das Neves, R. D. Adams, and J. K. Spelt, "Analytical models of adhesively bonded joints—Part I: Literature survey," *International Journal of Adhesion and Adhesives*, vol. 29, 2009, pp. 319–330.

[27] L. F. M. da Silva, P. J. C. das Neves, R. D. Adams, and J. K. Spelt, "Analytical models of adhesively bonded joints—Part II: Comparative study," *International Journal of Adhesion and Adhesives*, vol. 29, 2009, pp. 331–341.

[28] CalcBond, "Adhesive joint calculation software," [Online]. Available: https://app.calcbond.com/calcbond/index/. Accessed: 21-01-2025.

[29] N. F. Doğan, M. V. Çakır, and Ö. Özbek, "Bonding performance of nano boron nitride filled epoxy adhesive," *Journal of the Brazilian Society of Mechanical Sciences and Engineering*, vol. 46, 2024, Art. no. 240.

[30] M. V. Çakır, "The synergistic effect of hybrid nano-silica and GNP additives on the flexural strength and toughening mechanisms of adhesively bonded joints," *International Journal of Adhesion and Adhesives*, vol. 122, 2023, Art. no. 103333.